6th Congress of Alps-Adria
Acoustics Assosiation
16.-17. October 2014
Graz, Austria

Austrian Acoustics Association
Österreichische Gesellschaft für Akustik

Alps Adria Acoustics Association

ISBN: 978-3-200-03921-6

Comparison of acoustic resistance of a perforated plate absorber with a tightly and loosely placed thin porous layer

Ivan Vican, Kristian Jambrošić, Marko Horvat

University of Zagreb, Faculty of Electrical Engineering and Computing, Unska 3, 10000 Zagreb, Croatia
ivan.vican@fer.hr, kristian.jambrosic@fer.hr, marko.horvat@fer.hr

Abstract: *In this paper, the comparison of acoustic resistance of a perforated plate absorber for two characteristic cases is shown: one with a thin porous layer glued tightly to the backing of the perforated plate, and the other with a thin porous layer placed near the perforations, without tight contact. The measurements were done in the Kundt's tube, by using eight setups: four plates with different porosities (4.4%, 8.5%, 12.9% and 16.9%) and a 2 mm thick porous layer with two different air layer depths. The porous layer can simply be added to the acoustic resistance in the case of its tight placement to the perforated plate. On the other hand, absorber resistance is much less increased when a loosely placed porous layer is introduced to the perforations, but still shows a positive correlation with the resistance increase in the case of tight placement. Measured acoustic resistances are shown for two characteristic cases, including their numerical ratios between tight and loose contact. These ratios are introduced as an improvement to the analytical expression used for calculating the acoustic impedance, as well as an addition to the methods of tuning the acoustic resistance in complex absorber setups.*

Key words: perforated plate absorber; acoustic impedance; resonant absorber.

1. INTRODUCTION

Perforated plate absorbers are widely used for adjusting the reverberation time of spaces.

Due to their underlying physical principles, they usually work in a narrow frequency band. The most basic acoustic resonance can be achieved by using the Helmholtz resonator, which essentially consists of an air-filled cavity with a relatively small opening. The most common implementation of this structure is as a perforated plate resonator. Helmholtz resonator requires a smaller volume than porous absorbers in the frequency range they work most efficiently, but they also lack absorption due to small amount of energy dissipation. In order to achieve a more significant amount of sound absorption, damping (porous) material has to be added to the resonator cavity.

Although the impedance of a perforated plate in contact with air alone has been extensively researched by a number of authors [1-3], the amount of papers researching the impedance (especially resistance) of a perforated plate in contact with porous material is quite limited. For example, Selamet et al [4] and Lee et al [5] have done a number of researches concerning an increase in reactance when a porous layer is put in contact with the perforations. Models of acoustic resistance of a thin porous layer in contact with perforations were mostly developed by Ingard [6]. He added the porous layer resistance to the one induced by the viscosity of air in the perforations, gaining substantial increase in sound absorption in comparison to the case with no porous layer added. This “hard” contact stands for the case of porous material being placed near the perforations, within the distance of one orifice diameter, where the particle velocity of the sound wave still doesn’t go back to the uniform value after propagating from the orifices, as it had before entering the holes [7]. This paper demonstrates the validity of the model [6] in calculating acoustic resistance for the case when the porous layer is tightly glued to the perforated plate. Another case is introduced, namely when the mentioned layer is still in hard contact with the perforations (within the distance of one orifice diameter), but loosely placed near the perforations. For the latter setup it can be shown that the increase in resistance, compared to the case with no porous material added, is not as substantial as when the tightly placed porous layer is introduced. A validation of the mentioned hypothesis was done by measuring the sound absorption of 8 different samples for two characteristic cases.

2. IMPEDANCE CALCULATION

2.1. Perforated absorber setup and general impedance calculation

A typical perforated panel consists of 4 layers, with setup depicted in Fig. 1:

- perforated plate,
- thin porous absorber,
- air cavity,
- rigid backing.

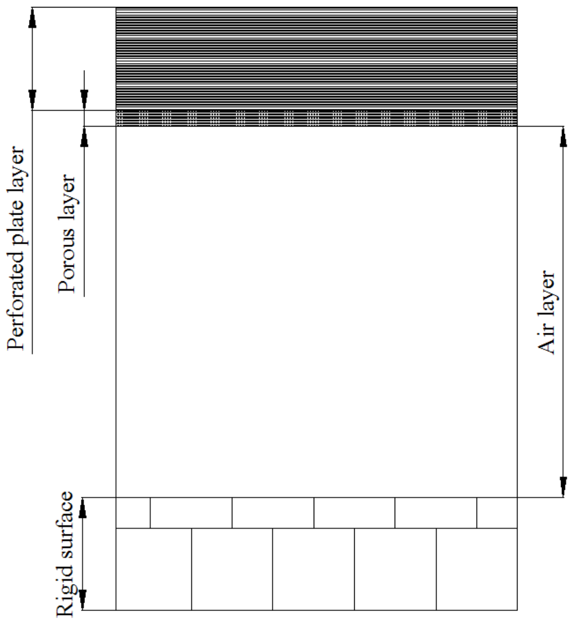

Fig. 1. Cross-section of the chosen setup.

Absorbing (porous) material may or may not be added, but in order to increase absorption, a layer of the material should be placed behind the perforations.
Acoustic impedance of various layers can easily be calculated using transfer matrices, with the solution:

$$Z_{si+1} = Z_i \frac{Z_{si}\cosh(\gamma_i d_i) + Z_i \sinh(\gamma_i d_i)}{Z_{si}\sinh(\gamma_i d_i) + Z_i \cosh(\gamma_i d_i)}, \qquad (1)$$

where

$$\gamma_i = jk_i. \qquad (2)$$

Z_i and k_i are the corresponding characteristic impedance and wavenumber of the i_{th} layer, respectively. The surface impedance is calculated for the top of the i_{th} layer, which is then used to calculate the impedance at the top of the $(i+1)_{th}$ layer. Z_{si} is the surface impedance at $x = x_i$; Z_{si+1} is the surface impedance at $x = x_{i+1}$.
The aforementioned acoustic layers are shown in Fig. 2.

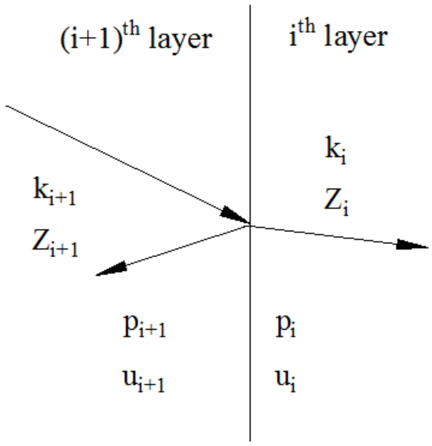

Fig. 2. Acoustic impedance and the wavenumber of bordering layers.

2.2. Impedance of air and porous layers

The impedance of the rigid backing layer is usually taken as $Z_{backing} = \infty$. Therefore, with known depth of the air layer d, its wave number ($k_{air} = \frac{\omega}{c}$), characteristic impedance of air Z_{air}, and the surface impedance of the previous layer (in this case, $Z_{backing}$), the air layer surface impedance can be calculated as:

$$Z_{s,air} = Z_{air} \frac{Z_{backing}\cosh(\gamma_i d_i) + Z_{air}\sinh(\gamma_i d_i)}{Z_{backing}\sinh(\gamma_i d_i) + Z_{air}\cosh(\gamma_i d_i)}, \qquad (3)$$

which yields

$$Z_{s,air} = -jZ_{air} cot(k_{air} d). \qquad (4)$$

It is obvious that the air layer adjacent to the rigid backing will be included only as a reactance.
For the porous layer, the characteristic impedance of the material, as well as its wave number, is not known *a priori*, as for the case of air impedance calculation. Two main models for the calculations are used (Delany-Bazley [8] and Allard-Champoux [9]), but require a length-specific flow resistivity parameter, defined as a pressure drop on the material of thickness *d*, with constant particle velocity *u*:

$$\sigma = \frac{p_2 - p_1}{ud}, \qquad (5)$$

and is expressed in *Rayl/m*, where 1 *Rayl* equals 1 $Ns/_{m^3}$.

The auxiliary term X is presented, incorporating air density ρ and frequency *f*:

$$X = \frac{\rho f}{\sigma}. \qquad (6)$$

The Allard-Champoux model for impedance and wave number of porous layer is given as:

$$Z_{porous} = Z_{air}[1 + 0.0571X^{-0.754} - j0.087X^{-0.732}], \quad (7)$$

$$k_{porous} = k_{air}[1 + 0.0978X^{-0.700} - j0.189X^{-0.595}]. \quad (8)$$

Surface impedance on top of porous and air layer is finally:

$$Z_a = Z_{porous}\frac{Z_{s,air}\cosh(k_{porous}d) + Z_{porous}\sinh(k_{porous}d)}{Z_{s,air}\sinh(k_{porous}d) + Z_{porous}\cosh(k_{porous}d)}. \quad (9)$$

For very thin layers of porous material, used for purposes of this paper, the porous layer calculations can be disregarded in this section, since its contribution will be added to the perforated plate impedance in subsection 2.4. For this reason impedance Z_a can be written as

$$Z_a = Z_{s,air} \quad (10)$$

in the case of porous material being very thin, or non-existent.

2.3. Impedance of perforated plate in contact with air alone

The specific acoustic impedance of a hole is defined as:

$$Z_h = \frac{p_1 - p_2}{u_h} = R + j\omega L_s = 4R_s(1 + \frac{t}{2r}) + jk\rho c l_{eff}, \quad (11)$$

where R_s is specific resistance, L_s the specific inertance, t is the thickness of the perforated plate and r is the radius of the hole on the plate. l_{eff} is defined as the effective length of the hole:

$$l_{eff} = t + 2\delta r, \quad (12)$$

with δ being the reactance end correction coefficient. The reason for this correction is that the mass of air in the hole consists not only of the mass in the hole itself, but also of air on both sides of the aperture.
Rayleigh [10] suggested the factor δ as

$$\delta = \frac{8}{3\pi}. \quad (13)$$

This correction factor only works for one hole in a plate, so Ingard [6] did an extensive research in which he considered two holes on a plate and their coupling. Fok [11] also researched the effect (known as “Hole interaction effect” – HIE), and Rschevkin [12] derived a modification to Rayleigh’s factor by using the so-called Fok function:

$$\psi(\varepsilon) = (1 + x_1\varepsilon + x_2\varepsilon^2 + x_3\varepsilon^3 + x_4\varepsilon^4 + x_5\varepsilon^5 + x_6\varepsilon^6 + x_7\varepsilon^7 + x_8\varepsilon^8)^{-1} \quad (14)$$

$$x_1 = -1.4092 \quad x_2 = 0 \quad x_3 = 0.33818 \quad x_4 = 0$$
$$x_5 = 0.06793 \quad x_6 = -0.02287 \quad x_7 = 0.03015$$
$$x_8 = -0.01641.$$

This modified correction factor now equals to $\frac{\delta}{\psi(\varepsilon)}$, where plate porosity ε can be taken as a ratio of hole and plate surfaces. It is apparent that this correction factor gets smaller with higher porosity, due to higher amount of air fluctuation in hole interaction.
Surface resistance of the plate, in the case of air being on both sides of the aperture, was also derived by Ingard [6]:

$$R_s = \frac{1}{2}\sqrt{2\mu\rho\omega}, \quad (15)$$

where μ is the viscosity of air, with a small value of $1.84 * 10^{-5}$ poiseuille. This is the reason why plate resistance (R) is almost negligible, and requires a (thin) layer of cloth, screen or other porous material to increase the overall resistance.
The pressure drop $p_1 - p_2$ is the same in the hole as well as on the plate itself, with different particle velocities, one being u_h in the hole and another being u_p on the plate. Their ratio can be extrapolated from the continuity equation:

$$u_p = \frac{A_h}{A_p}u_h = \varepsilon u_h, \quad (16)$$

where A_h is the surface area of holes and A_p the surface area of the whole plate.
Correspondingly, the overall plate impedance without adjacent porous material can be written as

$$Z_p = \frac{p_1 - p_2}{u_p} = \frac{4R_s(1 + \frac{t}{2r}) + jk\rho c l_{eff}}{\varepsilon}. \quad (17)$$

It is evident from Eq. (17) that the plate impedance can be greatly influenced by varying the porosity ε.

2.4. Impedance of perforated plate in contact with tightly placed thin porous layer

Resistance and reactance correction factors differ from the ones in subsection 2.3 when there is a (thin) porous layer adjacent to the plate.
Kirby and Cummings [3] suggested a semi-empirical formulation for the effect of a porous layer on hole reactance, which Lee et al [5] expanded by modifying effective hole length to

$$l'_{eff} = t + \frac{0.75}{2}\left(1 + \frac{Z_{porous}k_{porous}}{Z_{air}k_{air}}\right)2r. \qquad (18)$$

This particular reactance end correction of 0.75 was calculated for a porosity of 4.7%, but it is still a good approximation for most setups.
Ingard [6] stated that by "hard-facing" the porous layer to the plate (within a distance that equals the diameter of the hole), the resistance of the hole R can be greatly increased, by including the resistance of the mentioned porous material:

$$R_{tight} = 4R_s(\epsilon + \frac{t}{2r}), \qquad (19)$$

where

$$\epsilon = 1 + \frac{\sigma t'}{4R_s}. \qquad (20)$$

Once again, σ is flow resistivity per unit length of porous material and t' is the thickness of porous material.
It should be noted that although Morse and Ingard [13] proposed a dynamic flow resistivity parameter, that is weakly frequency dependent (proportional to $\sqrt{f}$). It is considered that in practice the static flow resistivity parameter σ is accurate enough for modeling in any acoustic regime [8].
The whole perforated plate impedance can now be modeled analogous to the previous subsection, which yields:

$$Z_p = \frac{4R_s(\epsilon + \frac{t}{2r}) + jk\rho c l'_{eff}}{\varepsilon}. \qquad (21)$$

In order to maximize the absorption, the term $\frac{\sigma t'}{\varepsilon}$ must be made as close as possible to the characteristic air impedance ρc.
Finally, the perforated plate impedance can simply be added to the one calculated at the top of porous layer:

$$Z_{all} = Z_p + Z_a. \qquad (22)$$

Eq. (22) corresponds both to subsections 2.3 and 2.4.

3. MEASUREMENTS

3.1. Measurements setup

All measurements were done in the Kundt's tube, in order to find the acoustic resistance and reactance, and consequently to calculate the absorption coefficients. 8 different samples were measured for two characteristic cases of porous layer placement, giving a total of 16 measurements. The sample setups (Table 1) included a porous layer (2 mm thick foam with 12000 Rayls/m flow resistivity), and a 15 mm thick perforated wooden plate with holes of 3 mm radius. This layout of the used perforations is shown in Fig. 3.

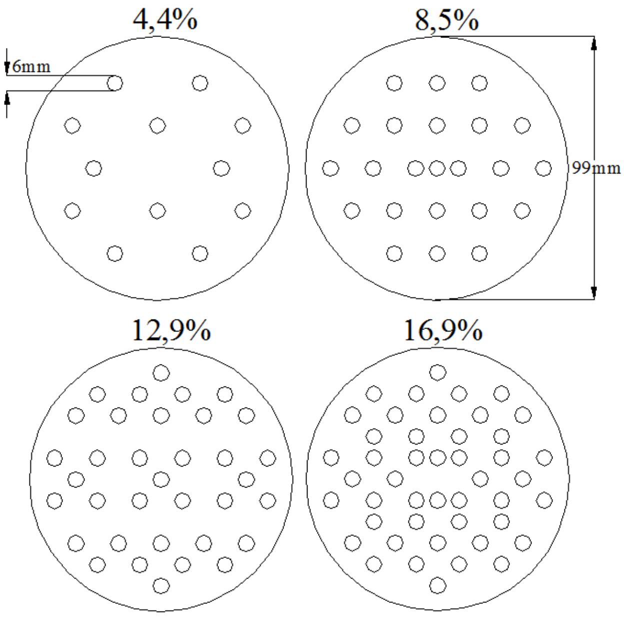

Fig. 3. Layout of perforated samples.

Table 1. Parameters of measured samples.

Setup designation	a)	b)	c)	d)	e)	f)	g)	h)
Perforated plate porosity	4.4%	4.4%	8.5%	8.5%	12.9%	12.9%	16.9%	16.9%
Air layer thickness [mm]	75	35	75	35	75	35	75	35

3.2. Comparison of calculated and measured absorption coefficients

In order to prove the validity of the mathematical model, the comparison of the absorption coefficient for calculated and measured acoustic impedance is given in Fig. 4. Due to the third-octave filtering (which is not as precise as e.g. 1/12-octave measurements) and errors in Kundt's tube measurements, an offset in resonant frequency and absorption of up to 10% was expected. The measurement curve shifts to lower frequencies when compared to simulated curves (with a relative maximum of 10%). Mathematically speaking, this manifests itself as an added mass to the sample (i.e. air layer thickness is larger than it appears).

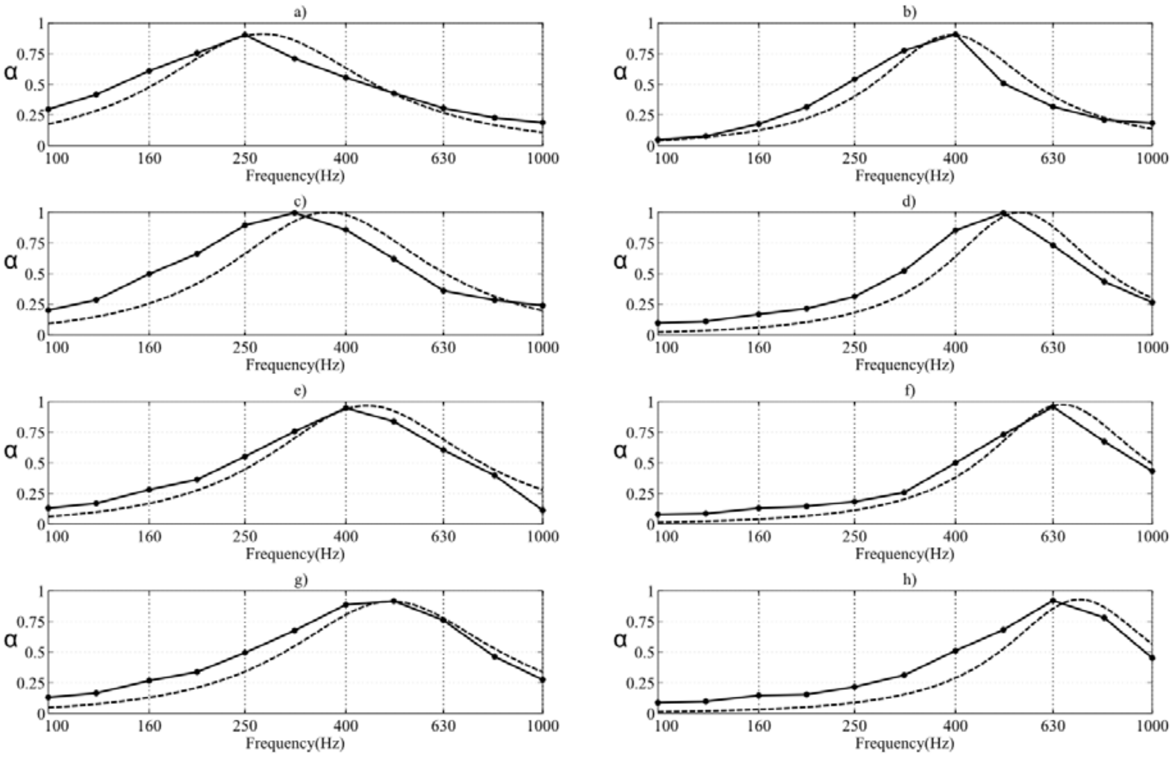

Fig. 4. Comparison of calculated and measured absorption coefficients. ———— measured, - - - - - - - calculated.

3.3. Comparison of measured absorption of samples with tightly and loosely placed porous layers

Fig. 5 shows the comparison of absorption for measured samples in the observed cases. As it can be seen, the samples with loosely placed porous layers show a significant drop in absorption, compared to the ones with tightly placed porous layers.

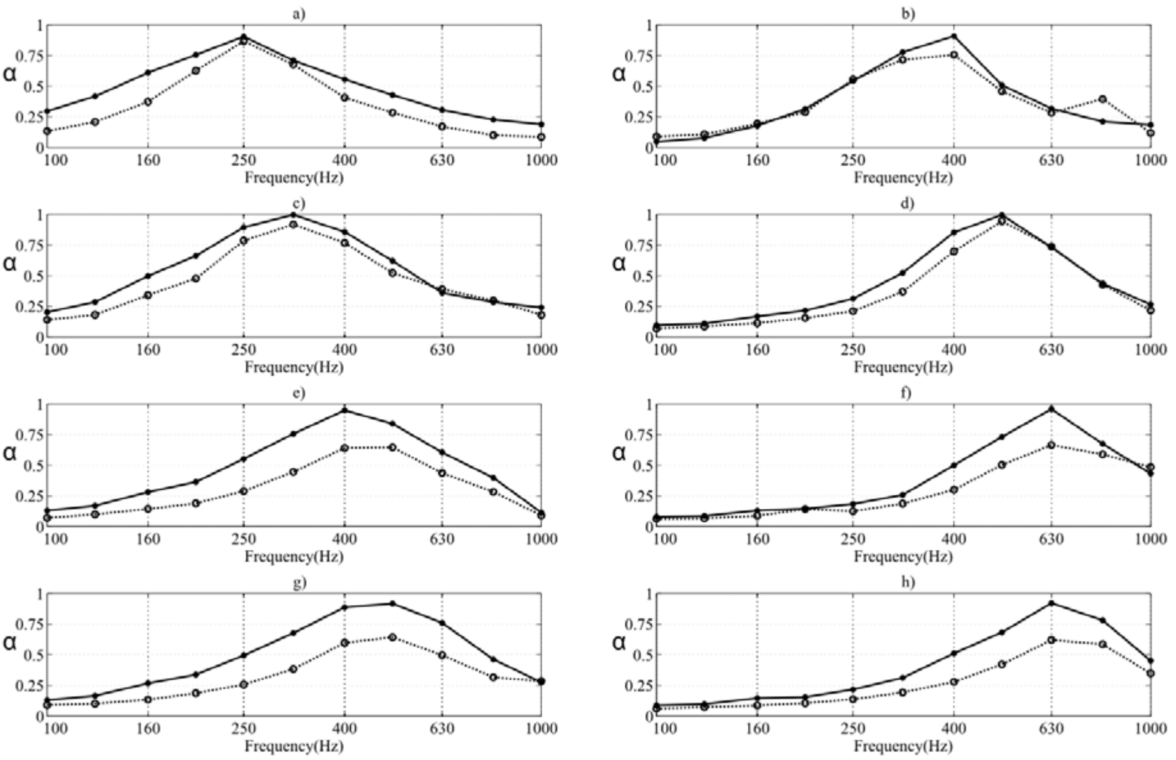

Fig. 5. Comparison of measured absorption of samples with tightly and loosely placed porous layers. ———— tight contact, ·············· loose contact.

3.4. Comparison of acoustic resistances of samples with tightly and loosely placed porous layers

Due to the fact that the compared cases have the same perforated plates and the same air layer thicknesses, the only change could have originated in the acoustic resistance of the samples, while maintaining the same reactance. Fig. 6 shows the comparison of acoustic resistances for observed cases with different porous material placement.

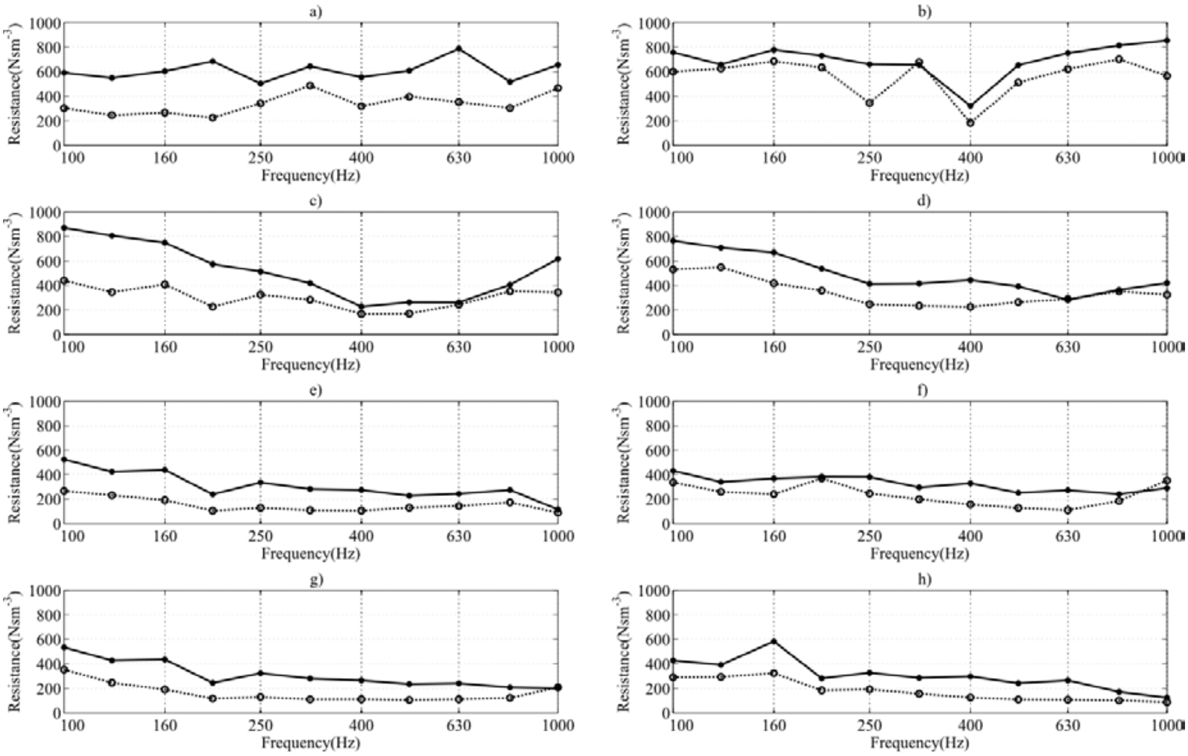

Fig. 6. Comparison of acoustic resistances of samples with tightly and loosely placed porous layers. ———— tight contact, ··········· loose contact.

Table 2 shows the ratios of acoustic resistance in tight and loose contacts over 11 frequency bands.

Table 2. Frequency dependent ratios of acoustic resistance for samples with tightly and loosely placed porous layers

	Acoustic resistance ratio k_r							
Frequency [Hz]	a)	b)	c)	d)	e)	f)	g)	h)
100	1.95	1.26	1.98	1.44	1.96	1.28	1.52	1.47
125	2.24	1.05	2.34	1.29	1.83	1.31	1.74	1.33
160	2.27	1.14	1.83	1.60	2.29	1.54	2.29	1.80
200	3.05	1.15	2.55	1.50	2.25	1.03	2.09	1.53
250	1.48	1.92	1.58	1.67	2.62	1.56	2.50	1.70
315	1.32	0.97	1.48	1.79	2.59	1.48	2.55	1.83
400	1.75	1.75	1.37	1.97	2.56	2.10	2.37	2.36
500	1.54	1.28	1.55	1.49	1.75	1.96	2.21	2.21
630	2.24	1.21	1.07	0.98	1.69	2.48	2.14	2.45
800	1.71	1.16	1.15	1.03	1.59	1.30	1.68	1.70
1000	1.40	1.51	1.80	1.30	1.28	0.82	0.96	1.43

4. CONCLUSIONS

The perforated plate resistance varies with the placement of the porous layer in regard to the adjacent perforated plate. It has been shown, for 4 porosities and 2 different air masses in the perforated absorber, that the acoustic resistance was reduced when incorporating loose contact, while the porous layer was still within the distance of one orifice diameter from the plate.

The model with the porous layer glued tightly to the plate was validated by comparing the measurements with the numerical model introduced in section 2. Absorption of the samples in tight contact was then compared to the absorption of samples in loose contact, and a significant reduction in the latter case was shown. The frequency dependent ratios of acoustic resistance values for two observed cases were shown in Table 2.

These ratios, which can be described as factors of reduction in acoustic resistance when moving from tight to loose contact, can be used as an important factor in absorber design, where minor changes in the placement of the porous layer (tight or loose) can increase the versatility of acoustic resistance values, thus giving a new approach in tuning the absorption characteristics of absorbers with the same geometry. A more extensive research, such as measurements including different porous layer thicknesses and taking into account the effects of diffuse sound field, is required in order to fully validate the results.

5. ACKNOWLEDGEMENTS

This research has been supported by the Croatian BICRO 5th Proof of Concept Program (Grant no. PoC5_1_83).

6. REFERENCES

[1] N. Atalla, F. Sgard, Modeling of perforated plates and screens using rigid frame porous models, *Journal of Sound and Vibration* 303 (2007) 195-208.

[2] T.H. Melling, The acoustic impedance of perforates at medium and high sound pressure levels, *Journal of Sound and Vibration* 29 (1973) 1-65.

[3] R. Kirby, A. Cummings, The impedance of perforated plates subjected to grazing gas flow and backed by porous media, *Journal of Sound and Vibration* 217 (1998) 619–636.

[4] A. Selamet, I.-J. Lee, Z.L. Ji, N.T. Huff, Acoustic attenuation performance of perforated concentric absorbing silencers, *SAE Noise and Vibration Conference and Exposition*, April 30–May 3, Traverse City, MI, SAE Paper No. 2001-01-1435 (Society of Automotive Engineers, Pennsylvania), 2001.

[5] I.-J. Lee, A. Selamet, N.T. Huff, Acoustic impedance of perforations in contact with fibrous material, *Journal of the Acoustical Society of America* 119 (2005) 2785–2797.

[6] U. Ingard, On the theory and design of acoustic resonators, *Journal of the Acoustical Society of America* 25 (1953) 1037–1061.

[7] U. Ingard, Noise Reduction Analysis, Jones and Bartlett (Sudbury, Massachusetts), 2010.

[8] M.E. Delany, E.N. Bazley, Acoustical properties of fibrous absorbent materials, *Applied Acoustics* 3 (1970) 105–116.

[9] J.F. Allard, Y. Champoux, New empirical equations for sound propagation in rigid frame fibrous materials, *Journal of the Acoustical Society of America* 91(6) (1992) 3346–3353.

[10] L. Rayleigh, Theory of sound, Macmillan (London), 1940.

[11] V.A. Fok, Teoreticheskoe issledovanie provodimosti kruglogo otverstiya v perogorodke, postavlennoi poperek truby (Theoretical study of the conductance of a circular hole, in a partition across a tube), *Doklady Akademii Nauk SSSR* 31(9) (1941) 875–878.

[12] S.N. Rschevkin, A Course of Lectures on the Theory of Sound, Pergamon Press (London), 1963.

[13] P.M. Morse, U. Ingard, Theoretical Acoustics, McGraw-Hill (New York), 1986.